Chalcogenide Letters Vol. 19, No. 7, July 2022, p.471 - 481

Luminescence thermometry based on downshifting and upconversion photoluminescence of $Bi_4Ti_3O_{12}:Yb^{3+}/Pr^{3+}$ ceramic

Z. Liu*, R. X. Wang
School of Science, Jinling Institute of Technology, Nanjing 211168, China

Yb^{3+}/Pr^{3+} codoped $Bi_4Ti_3O_{12}$ (abbreviated as $Bi_4Ti_3O_{12}:Yb^{3+}/Pr^{3+}$) ceramic was successfully fabricated by solid state sintering method. The structural, morphological and luminescence properties were investigated by X-Ray diffraction, scanning electron microscopy, steady-state downshifting and upconversion photoluminescence spectra. Green and red downshifting emissions can be effectively excited by 450 nm blue light irradiation. The intensity ratios of downshifting green and red emissions are sensitive to temperature. The spectral positions of downshifting green and red emissions show blue-shift with elevation of temperature. Under 980 nm excitation, the tempreature dependent upconversion photoluminescence were recorded. Based on fluorescence intensity ratio of 545 nm and 623 nm in upconversion emission spectra, temperature sensing was achieved with maximum absolute sensitivity value of 0.0068 K^{-1} at 443 K. These results show $Bi_4Ti_3O_{12}:Yb^{3+}/Pr^{3+}$ ceramic is a promising candidate for luminescence thermometry, which may find its applications in the scientific research and industry.

(Received April 15, 2022; Accepted July 20, 2022)

Keywords: Luminescence thermometry, Fluorescence intensity ratio, Spectral shift, Upconversion, Downshifting

1. Introduction

Temperature plays a crucial role in scientific research and industrial production. Many methods for temperature sensing have been widely investigated, including thermocouple, liquid expand, optical temperature sensing. Among them, the optical temperature sensing has drawn a lot of attention due to their advantages of real-time, rapid response, contact-less, durability in harsh environment [1, 2]. In recent years, the investigation on optical temperature sensing based on photoluminescence from rare earth ions (abbreviated as luminescence thermometry in this work) has been prevailing due to the abundant temperature dependent spectra of trivalent rare earth ions, resulting from their unique energy level structures. The luminescence thermometry often make use of spectral characteristic parameters, including absolute emission intensity, fluorescence intensity ratio, bandwidth of emission band, position of emission peak, fluorescence lifetime, as index to evaluate the variation of temperature [3-7]. Among these parameters, the utilizing of fluorescence intensity ratio can reduce the effects of unwanted fluctuations of excitation light source power on

* Corresponding author: liuzhen@jit.edu.cn
https://doi.org/10.15251/CL.2022.197.471

accurate measurement. Various luminescent active rare earths ions have been introduced for achieving temperature sensing based on their steady-state upconversion or downshifting photoluminescence upon appropriate wavelength excitation [8-12]. Trivalent praseodymium (Pr^{3+}) ions are attractive due to the green and red emissions can be generally obtained when excited by low-cost commercial blue LEDs (450 nm-470 nm) [13]. In addition, Pr^{3+} doped luminescent materials may exhibit strong environment sensitive photoluminescence which is suitable for applications in physical sensor field [14]. Trivalent ytterbium (Yb^{3+}) ions are commonly used sensitizers due to the high absorption cross section under typical 980 nm near-infrared light excitation, which is efficient to provide activators with enough energy for converting low-energy infrared light to high-energy visible light [15-17].

For rare earths doped luminescent materials, selecting an appropriate host material plays an important role for enhancing optical performance by providing dopant ions with desired crystal environment. Compared with fluorides and sulfides, the oxides have been found promising host materials due to their environment durability, physical and chemical stability and appropriate phonon energy [18, 19]. Ferroelectric oxides as host materials were reported for the integrated opto-electro-mechanical properties [20]. Bismuth titanate ($Bi_4Ti_3O_{12}$) is a typical Aurivillius ferroelectric oxide, which is composed of positive $(Bi_2O_2)^{2+}$ slabs and negative $(Bi_2Ti_3O_{10})^{2-}$ pseudo perovskite layers. By virtue of the advantages of high curie temperature and intrinsic ferroelectric properties, $Bi_4Ti_3O_{12}$ has been seen as an excellent choice for high temperature electrical devices [21]. Besides, through doping with metallic ions [22-26], conjugating with other compounds [27,28] and morphology engineering [29], the modified $Bi_4Ti_3O_{12}$ based materials exhibited outstanding piezoelectric, catalytic, optical performance. As far as we know, there is no report on luminescence thermometry based on upconversion and downshifting photoluminescence of Yb^{3+}/Pr^{3+} co-doped $Bi_4Ti_3O_{12}$ ($Bi_4Ti_3O_{12}:Yb^{3+}/Pr^{3+}$) ceramic.

In this work, the $Bi_4Ti_3O_{12}:Yb^{3+}/Pr^{3+}$ ceramic was synthesized via solid state reaction. The structural and morphological characteristics were investigated via X-Ray diffraction and scanning electron microscopy. The temperature sensitive upconversion photoluminescence upon 980 nm excitation and downshifting photoluminescence upon 450 nm excitation were systematically investigated through steady-state fluorescence spectra of synthesized sample at various temperature. Based on fluorescence intensity ratio and spectral shift analysis, the temperature sensing properties of $Bi_4Ti_3O_{12}:Yb^{3+}/Pr^{3+}$ ceramic were reported.

2. Experimental procedures

The $Bi_{4-x-y}Ti_3O_{12}:xYb^{3+}$, yPr^{3+} (x=0.02, y=0.005) ceramic was prepared by solid state reaction route. High pure Bi_2O_3 (Aladdin 99.9%), TiO_2 (Macklin 99.9%), Yb_2O_3 (Aladdin 99.9%), Pr_6O_{11} (Aladdin 99.9%) powders were selected as the raw materials. The lanthanide rare earth ions were designed to substitute the Bi^{3+} ions in lattice. Firstly, the raw materials were weighted according to the designed stoichiometric ratio. Subsequently, these raw materials were mixed and ground in agate mortar with alcohol for 2 h. After grinding, the obtained slurry was dried and calcined at 850 ℃ for 2 h in muffle furnace. After calcining, the temperature were naturally cooled down to obtain the $Bi_{4-x-y}Ti_3O_{12}:xYb^{3+}$, yPr^{3+} (x=0.02, y=0.005) powders. Then, the calcined powders were reground while adding 5% poly vinyl alcohol (PVA) solution as binder. After that,

0.5 g powders were uniaxially compressed in a steel mould with diameter of 13 mm to get circular pallet. Finally, the circular shaped pallet was burned out PVA binder at 550 ℃ for 30 min and sintered at 980 ℃ for 2 h in muffle furnace and subsequently cooled down to room temperature to get the ceramic.

The phase structure of the ceramic sample was characterized by X-Ray diffraction technique (XRD, D/max 2400, Rigaku Corp., CuKα1 radiation at 0.154 nm, operating at 40 kV, 30 mA). Scanning electron microscope (Quanta FEG 250) was used to record the microscopic morphology and investigate the grain characteristics. The upconversion photoluminescence spectra of sintered sample were collected by fluorescence spectrometer (Edinburgh Instruments FLS980) equipped with photomultiplier tubes (PMT) detector. For the upconversion photoluminescence measurement, the power tunable 980 nm commercial diode laser was used as excitation light source. The downshifting photoluminescence excitation spectra and photoluminescence emission spectra were recorded by steady-state fluorescence spectrometer (Perkin Elmer FL8500) equipped a Xenon lamp excitation light source.

3. Results and discussion

Fig. 1 shows the XRD pattern of synthesized ceramic in the 2θ range from10° to 80°. The diffraction peaks can be matched well with the standard diffraction data of $Bi_4Ti_3O_{12}$ (PDF#73-2181), suggesting the doped ceramic maintain host structure. No secondary phase occurs in the diffraction pattern, demonstrating the doped rare earth ions have successfully incorporated into the host crystal lattice. The dominant diffraction peak around 30° is corresponded to the (117) crystal face, indicating the nature of layer arrangement of positive $(Bi_2O_2)^{2+}$ slabs and negative $(Bi_2Ti_3O_{10})^{2-}$ pseudo perovskite layers in the doped $Bi_4Ti_3O_{12}$ based Aurivillius ceramic [30]. Fig. 2 is the scanning electron microscopic image of surface of $Bi_4Ti_3O_{12}$:Yb^{3+}/Pr^{3+} ceramic. It can be clearly seen that the grains of $Bi_4Ti_3O_{12}$:Yb^{3+}/Pr^{3+} ceramic are plate-like slabs with thickness of about 50 nm. These plate-like grains of ceramic sample arrange irregularly, which is characteristic of layered Arrivillius ceramic without preferred orientation.

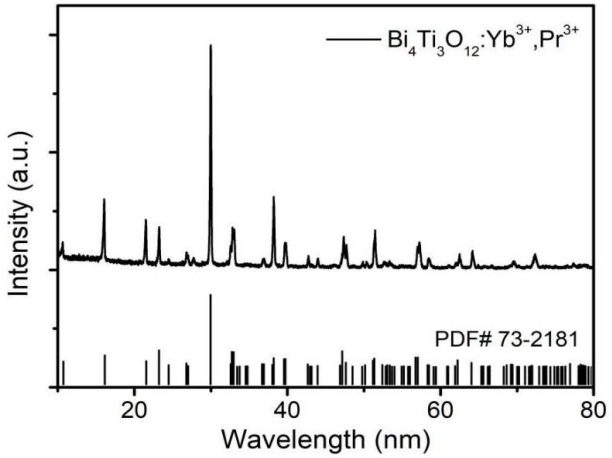

Fig. 1. X-Ray diffraction patterns of synthesized $Bi_4Ti_3O_{12}$:Yb^{3+}/Pr^{3+} ceramic.

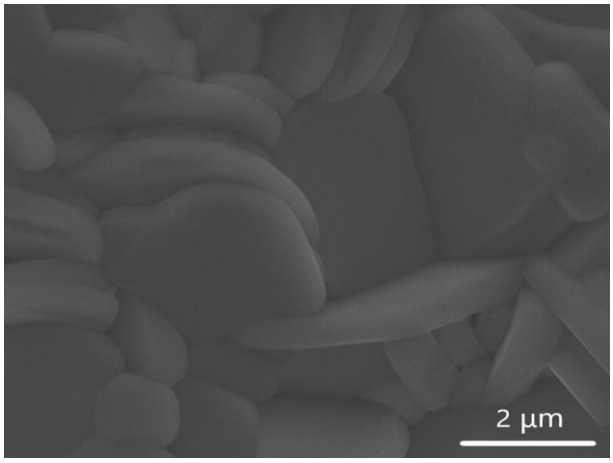

Fig. 2. Scanning electron microscopic image of synthesized $Bi_4Ti_3O_{12}:Yb^{3+}/Pr^{3+}$ ceramic.

The excitation spectra of $Bi_4Ti_3O_{12}:Yb^{3+}/Pr^{3+}$ ceramic monitored at 623 nm is shown in Fig. 3. It can be obviously seen that excitation spectra in spectroscopic range from 420 nm to 510 nm contains three dominant bands peaked at 450 nm, 476.5 nm and 491.6 nm, attributing to transitions of $^3H_4 \rightarrow {}^3P_2$ (Pr^{3+}), $^3H_4 \rightarrow {}^3P_1$ (Pr^{3+}) and $^3H_4 \rightarrow {}^3P_0$ (Pr^{3+}), respectively. The band peaked at 450 nm shows the maximum intensity, suggesting the downshifting photoluminescence of synthesized ceramic can be effectively excited by 450 nm. For investigating the temperature sensing properties based on downshifting photoluminescence of $Bi_4Ti_3O_{12}:Yb^{3+}/Pr^{3+}$, the steady-state emission spectra at various temperature were collected. The temperature dependent downshifting photoluminescence emission spectra are shown in Fig. 4., which show two main emission bands. According to energy levels of Pr^{3+} [31], it can be concluded the green emission band located near 536 nm is corresponded with $^3P_{1,0} \rightarrow {}^3H_5$ (Pr^{3+}) transitions and red emission band located near 623 nm is corresponded with hybrid $^1D_2 \rightarrow {}^3H_4$ (Pr^{3+}), $^3P_0 \rightarrow {}^3H_6$ (Pr^{3+}) and $^3P_0 \rightarrow {}^3F_2$ (Pr^{3+}) transitions. The intensities of green and red emissions decrease obviously with elevation of temperature, indicating the downshifting emissions are sensitive to variation of temperature. In addition, the attenuation for green and red emission bands exist different trends. The fluorescence intensity ratios between integral intensities of green and red emission bands as a function of temperature are shown in Fig.5.

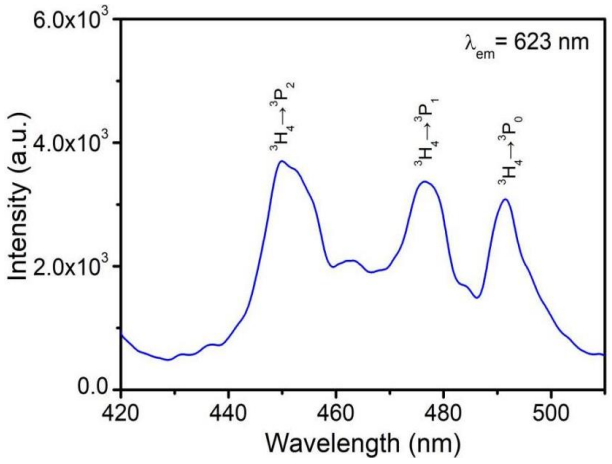

Fig. 3. Excitation spectra of $Bi_4Ti_3O_{12}:Yb^{3+}/Pr^{3+}$ ceramic monitored at 623 nm emission.

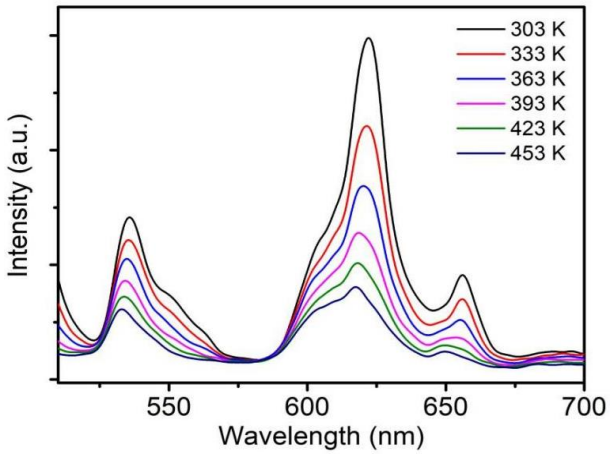

Fig. 4. Temperature dependent downshifting emission spectra of $Bi_4Ti_3O_{12}:Yb^{3+}/Pr^{3+}$ ceramic upon 450 nm excitation.

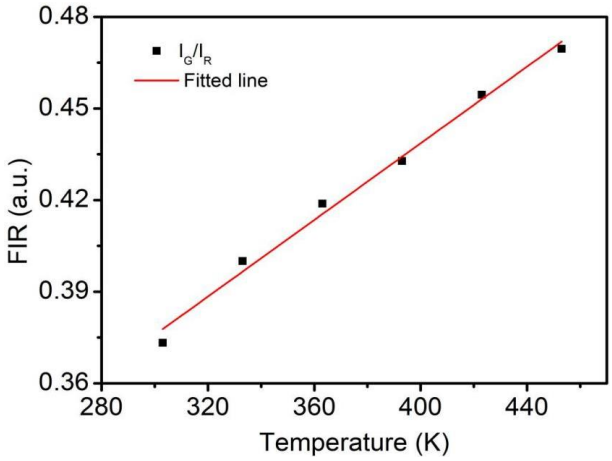

Fig. 5. Fluorescence intensity ratios between integral intensities of green and red emission bands (I_G/I_R) as a function of temperature.

As shown in Fig.5, the experimental data of temperature dependent fluorescence intensity ratios can be fitted by a linear function ($FIR = 6.275 * T + 0.188$). For quantitatively evaluating the temperature sensing properties, absolute sensitivity S_a can be calculated by the followed equation,

$$S_a = \left|\frac{dFIR}{dT}\right| \quad (1)$$

It can be calculated that absolute sensitivity for luminescence thermometry based on fluorescence intensity ratios of downshifting photoluminescence of $Bi_4Ti_3O_{12}:Yb^{3+}/Pr^{3+}$ is a constant, which is useful for practical application.

Fig. 6 shows the temperature dependent downshifting emission spectra of $Bi_4Ti_3O_{12}:Yb^{3+}/Pr^{3+}$ in the spectroscopic range of 520-560 nm, the positions of emission peak

exhibits blue-shift obviously, suggesting spectral shift of green emission is sensitive to variation of temperature. Fig. 7 shows the positions (X) of corresponding emission peak as a function of temperature from 303 K to 453 K. The experimental data can be fitted by a linear function $X = -0.0185 * T + 541.484$. The downshifting photoluminescence spectra of red emission in range of 580-650 nm at various temperature is shown in Fig. 8, exhibiting blue shift as increasing temperature in the range from 303 K to 453 K. Fig. 9 shows the spectral positions as a function of temperature, which can be fitted by $X = -0.0337 * T + 632.377$. These results show the spectral shift of green emission or red emission can be used in linear temperature sensing. The absolute sensitivity can be calculated by the following equation，

$$S_a = \left|\frac{dX}{dT}\right| \quad (2)$$

It indicates the spectral shift based luminescence thermometry of $Bi_4Ti_3O_{12}:Yb^{3+}/Pr^{3+}$ has constant absolute sensitivity. Combining with fluorescence intensity ratio based thermometry, dual-mode temperature sensing based on downshifting emission of $Bi_4Ti_3O_{12}:Yb^{3+}/Pr^{3+}$ can be achieved.

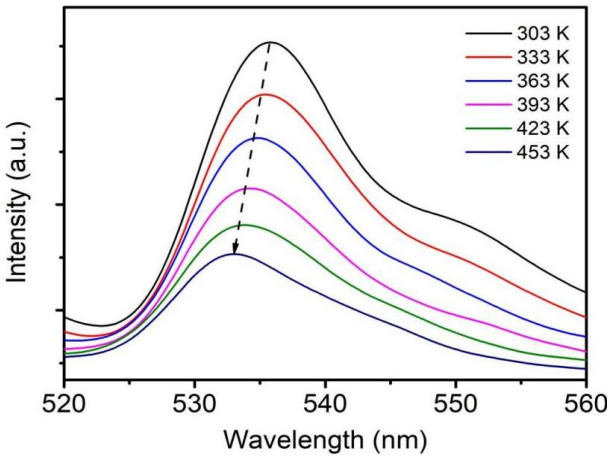

Fig. 6. Temperature dependent downshifting emission spectra of $Bi_4Ti_3O_{12}:Yb^{3+}/Pr^{3+}$ in the spectroscopic range of 520-560 nm.

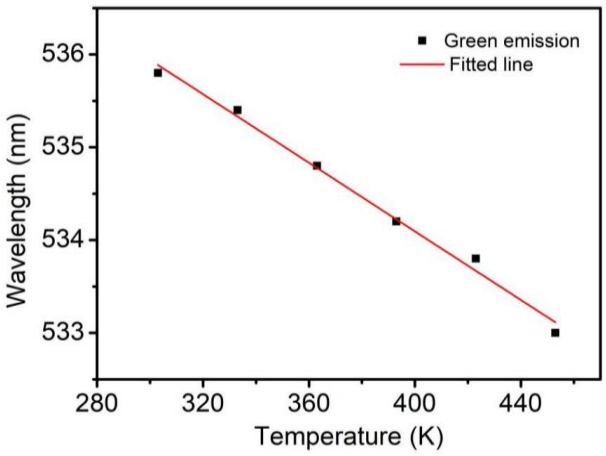

Fig. 7. Spectral positions of green emission as a function of temperature from 303 K to 453 K.

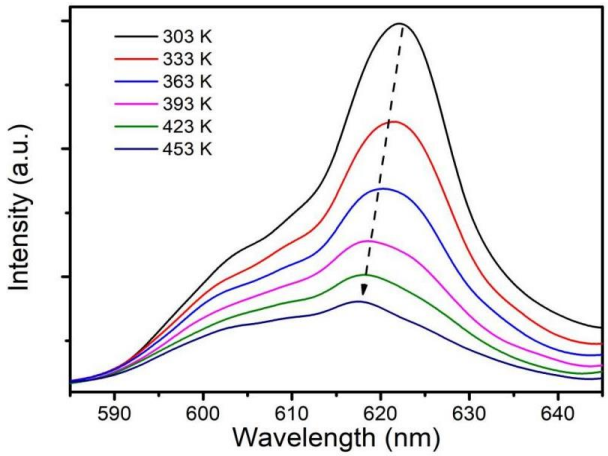

Fig. 8. Temperature dependent downshifting emission spectra of $Bi_4Ti_3O_{12}:Yb^{3+}/Pr^{3+}$ ceramic in the spectroscopic range of 580-650 nm.

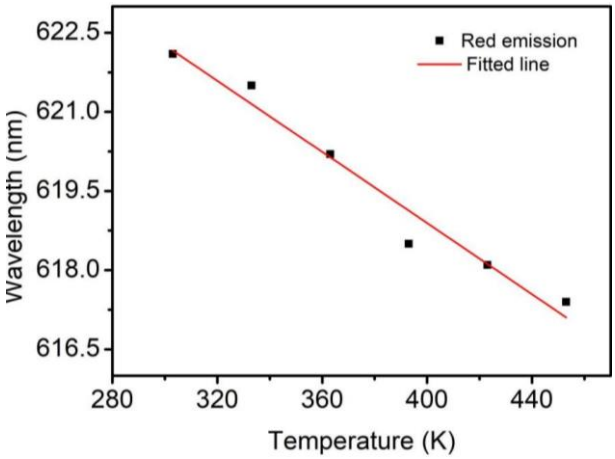

Fig. 9. Spectral positions of red emission as a function of temperature from 303 K to 453 K.

In order to investigate temperature sensing based on upconversion photoluminescence of $Bi_4Ti_3O_{12}:Yb^{3+}/Pr^{3+}$ ceramic, its temperature dependent emission spectra upon 980 nm excitation were recorded. Fig.10 shows the upconversion emission spectra of sample at various temperature. Three emission bands located at 545 nm, 623 nm and 658 nm were detected in spectroscopic range of 520 nm to 700 nm, respectively. The intensities of three emission bands decrease with increment of temperature. Fig.11 exhibits the fluorescence intensity ratio as a function of temperature. The experimental data can be well fitted by the exponential function (FIR=270.62*exp(-2801/T)+1.63). The absolute sensitivity curve calculated through Eq.1 is shown in Fig.12. Results suggest the maximum absolute sensitivity of luminescence thermometry based on upconversion photoluminescence of $Bi_4Ti_3O_{12}:Yb^{3+}/Pr^{3+}$ is 0.0068 K^{-1} at 443 K in measured temperature range.

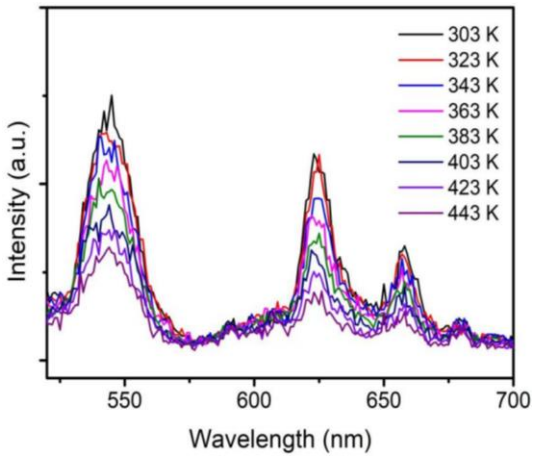

Fig. 10. Upconversion emission spectra of sample at various temperature in the range from 303 K to 443 K.

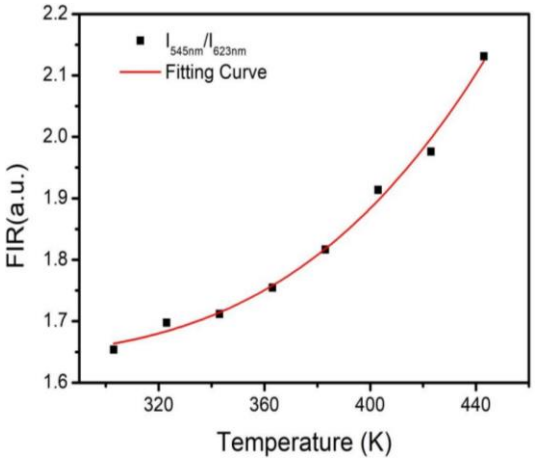

Fig. 11. Fluorescence intensity ratios (I_{545nm}/I_{623nm}) as a function of temperature.

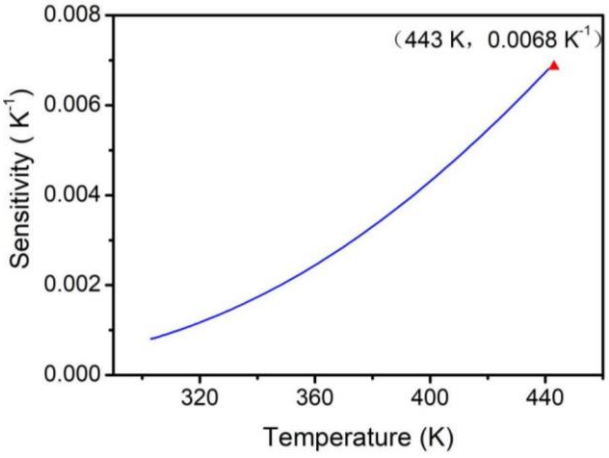

Fig. 12. Temperature dependent sensitivity curve of FIR based upconversion luminescence thermometry.

4. Conclusion

Yb^{3+}/Pr^{3+} codoped $Bi_4Ti_3O_{12}$ ceramic was successfully synthesized by solid state reaction method. XRD and SEM demonstrated the synthesized ceramic maintain layered perovskite structure after doping. Upconversion and downshifting photoluminescence of synthesized $Bi_4Ti_3O_{12}:Yb^{3+}/Pr^{3+}$ are sensitive to variation of temperature. The fluorescence intensity ratio of downshifting green and red emission is linearly change with variation of temperature. Meanwhile, spectral positions of green and red emissions exhibit linear blue-shift with elevation of temperature. Combining the fluorescence intensity ratio with spectral shift of downshifting emission, dual-mode temperature sensing is achieved in $Bi_4Ti_3O_{12}:Yb^{3+}/Pr^{3+}$ ceramic. Based on fluorescence intensity ratio of upconversion emission at 545 nm and 623 nm, the maximum absolute sensitivity of 0.0068 K^{-1}. All these results indicate the $Bi_4Ti_3O_{12}:Yb^{3+}/Pr^{3+}$ ceramic has great potential for application in luminescence thermometry.

Acknowledgements

This work is financially supported by the Research Start-up Program of Jinling Institute of Technology (jit-b-202054), the National Natural Science Foundation of China (Grant No.11804150), Natural Science Foundation of Jiangsu Province (BK20201111).

References

[1] W. Zheng, B.Y. Sun, Y.M. Li, R. Wang, ACS Applied Nano Materials 4 3922 (2021); https://doi.org/10.1021/acsanm.1c00303

[2] K. Okabe, N. Inada, C. Gota, Y. Harada, T. Funatsu, S. Uchiyama, Nature Communications 3 705 (2012); https://doi.org/10.1038/ncomms1714

[3] Z. Liu, G. C. Jiang, R. X. Wang，C. K. Chai, L. M. Zheng, Z.G.Zhang, B.Yang, W.W.Cao, Ceramics International 42 11309 (2016)

[4] Q. Wang, M. Liao, Q. M. Lin, M. X. Xiong, Z. F. Mu, F. G. Wu, Journal of Alloys and Compounds 850 156744 (2021); https://doi.org/10.1016/j.jallcom.2020.156744

[5] A. S. Laia, D. H. Hora, M. V. S. Rezende, Y. T. Xing, J. J. RodriguesJr., G. S. Maciel, M. A. R. C.Alencar, Journal of Luminescence 227 117524 (2020); https://doi.org/10.1016/j.jlumin.2020.117524

[6] G. C. Jiang, X. T. Wei, S. S. Zhou, Y. H. Chen, C. K. Duan, M.Yin, Journal of Luminescence 152 156 (2014); https://doi.org/10.1016/j.jlumin.2013.10.027

[7] H. Zhang, Y. J. Liang, H. Yang, S. Q. Liu, H. R. Li, Y. M. Gong, Y. J. Chen, G. G. Li, Inorganic Chemistry 59 14337 (2020); https://doi.org/10.1021/acs.inorgchem.0c02118

[8] H. Suo, X. Q. Zhao, Z. Y. Zhang, T. Li, E. M. Goldys, C. F. Guo, Chemical Engineering Journal 313 65 (2017); https://doi.org/10.1016/j.cej.2016.12.064

[9] H. Lin，D. K. Xu, Y. J. Li, L. Yao, L. Q. Xu, Y. Ma, S. H. Yang, Y. L. Zhang, Journal of Luminescence 216 116731 (2019); https://doi.org/10.1016/j.jlumin.2019.116731

[10] H. Suo, X. Zhao, Z. Zhang, C. Guo, Chemical Engineering Journal 389 124506 (2020); https://doi.org/10.1016/j.cej.2020.124506

[11] J. Zhang, J. J. Chen, F. S. Qian, Y. N. Zhang, S. S. An, Optics and Laser Technology 138 106854 (2021); https://doi.org/10.1016/j.optlastec.2020.106854

[12] P. Bolek, J. Zeler, C. D.S. Brites, J. T. Piegza, L. D. Carlos, E. Zych, Chemical Engineering Journal 421 129764 (2021); https://doi.org/10.1016/j.cej.2021.129764

[13] H. Sun, D. Peng, X. Wang, M. Tang, Q. Zhang, Journal of Applied Physics 111 046102 (2012); https://doi.org/10.1063/1.3686193

[14] Y. L. Qin, F. X. Han, P. K. Yan, Y. Q. Wang, Y. C. Zhang, S. J. Zhang, Ceramics International 47 24092 (2021); https://doi.org/10.1016/j.ceramint.2021.05.119

[15] F. Tang, H. Q. Li, K. Z. Tian,J. Q. Ning, H. G. Ye, S. J. Xu, Optics Letters 45 5712 (2020); https://doi.org/10.1364/OL.408308

[16] Y. B. Wang, H. Y. Li, H. Ma, L. Huang, Journal of Rare Earths 39 1477 (2021); https://doi.org/10.1016/j.jre.2021.04.007

[17] M. Back, E. Trave, P. Riello, J. J. Joos, The Journal of Physical Chemistry C 122 7389 (2018); https://doi.org/10.1021/acs.jpcc.8b00637

[18] W.P. Zhou, C. Y. Ma, C. L. Ma, Z. Y. Zhai, W. S. Tan, Journal of Luminescence 240 118419 (2021)

[19] Y. Y. Zhang, R. Q. Chu, Z. J. Xu, S. Z. Zhang, C. Zhang, G. R. Li, Ceramics International 47 30938 (2021); https://doi.org/10.1016/j.ceramint.2021.07.279

[20] X. Wang, C. N Xu, H. Yamada, K. Nishikubo, X. G. Zheng, Advanced Materials 17 1254 (2005); https://doi.org/10.1002/adma.200401406

[21] Y. X. Tang, Z. Y. Shen, Q. X. Du, X. Y. Zhao, F. F. Wang, X. M. Qin, T. Wang, W. Z. Shi, D. Z. Sun, Z. Y. Zhou, S. J. Zhang, Journal of the European Ceramic Society 38 5348 (2018); https://doi.org/10.1016/j.jeurceramsoc.2018.08.025

[22] X. D. Li, Z. N. Chen, L. S. Sheng, L. L. Li, W. F. Bai, F. Wen, P. Zheng, W. Wu, L. Zheng, Y. Zhang, Journal of the European Ceramic Society 39 2050 (2019); https://doi.org/10.1016/j.jeurceramsoc.2019.01.042

[23] Y. X. Tang, Z. Y. Shen, Q. X. Du, X. Y. Zhao, F. F. Wang, X. M. Qin, T. Wang, W. Z. Shi, D. Z. Sun, Z. Y. Zhou, S. J. Zhang, Journal of the European Ceramic Society 38 5348 (2018); https://doi.org/10.1016/j.jeurceramsoc.2018.08.025

[24] H. Chen, G. X. Bai, Q. H. Yang, Y. J. Hua, S. Q. Xu, L. Chen, Journal of Luminescence 221 117095 (2020); https://doi.org/10.1016/j.jlumin.2020.117095

[25] E. Pan, G. X. Bai, L. J. Wang, L. Lei, L. Chen, S. Q. Xu, ACS Applied Nano Materials 2 7144 (2019); https://doi.org/10.1021/acsanm.9b01631

[26] R. Bokolia, M. Mondal, V. K. Rai, K. Sreenivas, Journal of Applied Physics 121, 084101 (2017); https://doi.org/10.1063/1.4977006

[27] C. L. Liu, J. J. Xu, J. F. Niu, M. D. Chen, Y. H. Zhou, Separation and Purification Technology 241 116622 (2020); https://doi.org/10.1016/j.seppur.2020.116622

[28] K. Das, R. Bariki, D. Majhi, A. Mishra, K. K. Das, R. Dhiman, B. G. Mishra, Applied Catalysis B: Environmental 303 120902 (2022); https://doi.org/10.1016/j.apcatb.2021.120902

[29] Y.Z. Zhang, Z.W. Chen, Z. Y. Lu, Nanomaterials 8 261 (2018);

https://doi.org/10.3390/nano8040261

[30] X. Du, I. W. Chen, Journal of the American Ceramic Society 81 3260 (1998); https://doi.org/10.1111/j.1151-2916.1998.tb02765.x

[31] Z. Liu, R. X. Wang, D. H. Chen, Journal of Materials Science: Materials in Electronics 33 3748 (2022); https://doi.org/10.1007/s10854-021-07566-y